Centerline Kármán "Constant" Revisited And Contrasted To Log-layer Kármán Constant At CICLoPE

H. M. Nagib[1*], P. A. Monkewitz[2], L. Mascotelli[3], T. Fiorini[3], G. Bellani[3], X. Zheng[3] and A. Talamelli[3]

1: MMAE Department, Illinois Inst. Technology, Chicago, IL 60616, USA.
2: Faculty of Engr. Science, Swiss Federal Inst. Technology Lausanne, CH-1015 Lausanne, Switzerland.
3: Dept. of Industrial Engr., University of Bologna, 47100 Forli, Italy.
*Corresponding author: nagib@iit.edu

ABSTRACT

In early pipe flow experiments, the emphasis has been on the scaling of the centerline velocity and the friction factor with Reynolds number. As measurement techniques have evolved, attention has shifted towards the "law of the wall" $U^+ = (1/\kappa_{\rm wall})\ln(y^+) + B$ and its Kármán constant $\kappa_{\rm wall}$. In the last years the value of $\kappa_{\rm wall}$ in pipes has closely approached the "most popular" value of 0.384 for the zero-pressure-gradient boundary layer (Furuichi *et al.* (2015), Örlü *et al.* (2016)) which seemingly supports the claim of Marusic *et al.* (2013) that $\kappa = 0.39$ is universal for pipe flow and zero-pressure-gradient boundary layers.

However, the asymptotic matching to the "wake", already discussed by Coles (1956), has not received enough attention. It requires that $\kappa_{\rm wall}$ be the same as $\kappa_{\rm CL}$ in the expression for the centerline velocity $U^+_{\rm CL} = (1/\kappa_{\rm CL})\ln({\rm Re}_\tau) + C$, but $\kappa_{\rm CL}$ has consistently remained larger than 0.42. Only very recently Monkewitz (2017)) has proposed a resolution of this conundrum by introducing a **universal** internal wall log-law with $\kappa_{\rm int} = 0.384$ for the range $10^2 \lessapprox y^+ \lessapprox 10^3$, followed by an external log-law with $\kappa_{\rm ext} = \kappa_{\rm CL}$ for $y^+ \lessapprox 0.05{\rm Re}_\tau$ and the wake. The analysis of Monkewitz (2017) for pipe flow was based on the Superpipe data where $\kappa_{\rm ext} = 0.42$. So the question arises whether the difference between $\kappa_{\rm int}$ and $\kappa_{\rm ext}$ is statistically significant. The purpose of this contribution is to show that this is indeed the case, as $\kappa_{\rm CL}$ in CICLoPE is found to be $\mathbf{0.446 \pm 0.008}$. Interestingly, this value is very close to the original $\kappa_{\rm CL} = 0.436$ of Zagarola & Smits (1998) for the Superpipe and the value of 0.437 found in the first CICLoPE experiments by Fiorini (2017).

I. INTRODUCTION

The recently completed long pipe and large diameter facility in Predappio, Italy, operating with air at atmospheric conditions, was designed to provide high spatial resolution and stable operating conditions at high Reynolds numbers. Figure 1 clarifies the need for the large diameter without lowering the fluid viscosity to reach the Reynolds numbers where the asymptotic regime of wall-bounded turbulence can be experimentally investigated in the only geometry with homogeneous and symmetric boundary conditions. The 0.9 m diameter pipe has a length of over 120 diameters. The CICLoPE (Center for International Cooperation in Long Pipe Experiments) facility is depicted in Fig. 2, and the majority of the measurements reported here were carried out in the test section labeled a) in the lower part of the figure. This unique Center and its Long-Pipe facility, is hosted by the University of Bologna

The first sets of experiments carried out in this facility were recently reported by Örlü *et al.* (2016) and Fiorini (2017). The work reported here was carried out in a coordinated and complementary way with the analysis of Monkewitz (2017), "revisiting the quest for a universal log-law and the role of pressure gradient in "canonical" wall-bounded turbulent flows", by reanalyzing the mean velocity data from the Superpipe Zagarola & Smits (1998), and some channel flow data.

Both Örlü *et al.* (2016) and Fiorini (2017) report values for the Kármán constant in the logarithmic region of their profiles around 0.39 to 0.40. However, the range of their profiles did not extend beyond y^+ of 10^4, due to the limitations of the traversing mechanism they used. We consider and and will consistently label this Kármán constant as $\kappa_{\rm int}$. This value is very close to well established κ value of 0.384 for Zero-Pressure-Gradient (ZPG) boundary layers; see e.g., Monkewitz *et al.* (2007).

In the work of Fiorini (2017) a different traversing mechanism was used to obtain complete velocity profiles across the full section of the pipe and is shown here in Fig. 3. He also used a Pitot-static probe shown in the left-side of Fig. 4 to monitor the centerline velocity at various locations near the "test section." To estimate the wall shear stress in the test section region, he measured the static-pressure gradient along the fully developed section of the pipe, where a constant gradient is expected. Figure 5 and its caption clearly outline the approach used by Fiorini (2017), and indicates that in the CICLoPE facility at the Reynolds numbers investigated so far, the fully developed conditions may already exist beyond around 50 pipe diameters from the entrance. Fiorini (2017) presented data such as those reproduced here in Figs. 6 and 7 in an effort to demonstrate the validity of such a conclusion and the accuracy of the wall shear stress values extracted from them, with the aid of the fluid properties, i.e., temperature, pressure and humidity.

Fiorini (2017) in his thesis only focused on the mean velocity profiles in a region between the wall and 30% of the pipe radius, but he collected also some centerline velocities as a function of Reynolds number that are reported here with the recently acquired measurements. Typical mean velocity profiles from Fiorini (2017) are reproduced here in Fig. 8, and his best fit for his inner region of the log-law is $\kappa_{\rm int} = 0.399$ and $B = 4.50$. We note however, that the fit by Fiorini (2017) includes, in varying degree with the Reynolds number, both the interior and part of the exterior logarithmic regions identified by Monkewitz (2017). As a consequence, his κ represents some kind of an "average" between the two κ's.

II. PITOT PROBES

At the start of the current measurements, and with input based on the work of Fiorini (2017), we focused on improving on few aspects of the experimental arrangements and measurements. They included: the elimination of any deflection of the Pitot probes and any vibrations they may experience, especially at the highest flow speeds; the reduction of errors and uncertainty in the crucial pressure-gradient measurements along the fully developed part of the pipe; and possible improvement in the Pitot probe. Different experimental set-ups were tested in terms of Pitot tube diameter, location, blockage effect and static pressure holes to measure the centerline velocity in a fully developed turbulent pipe flow in the CICLoPE Long Pipe (see Fiorini (2017) for a full description of the facility). The Re_τ values explored ranged from 8×10^3 to 40×10^3.

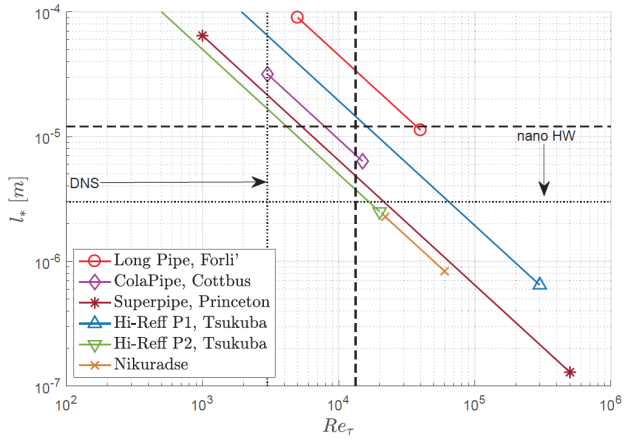

Figure 1. Viscous length scale as a function of friction Reynolds number for various pipe flow facilities, indicating ranges of good spatial resolution; Reproduction of Figure 2.1 of Fiorini (2017).

The data were sampled at 5Hz over a 1 minute period.

For each case, the position of the Pitot probe was checked to be within 1mm of the centerline. A preliminary investigation of the behavior of the probes at different velocities was carried out, to look for possible deflections or vibrations. A glass window was inserted at the probe location for this purpose. For the first probe tested, vibrations were detected from medium to high Reynold numbers, therefore, a support was added to the stem as shown in the left part of Fig.4. A different behavior was observed for the second and the third probe, which were supported by the traversing mechanism of Fig. 3 as shown in Fig. 4, where no deflection or vibration was noted. In the next paragraphs a description of each set-up will be presented.

To evaluate and benchmark the various centerline measurements and Pitot probes, we utilized the pressure drop from the contraction entrance to the pipe and the flow average or bulk velocity

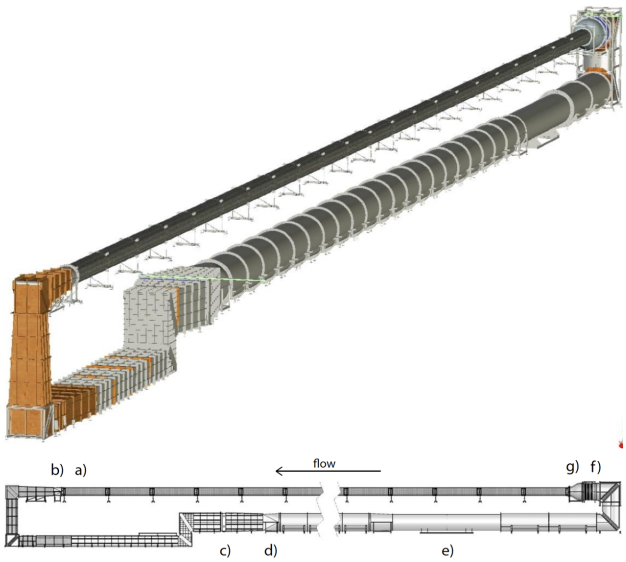

Figure 2. Visual and schematic representations of the CICLoPE pipe; a) Measuring station. b) Round to rectangular shape converter. c) Heat exchanger. d) Rectangular to round shape converter. e) Axial fans. f) Flow conditioning section (honeycomb, screens). g) Contraction section with ratio of 4.

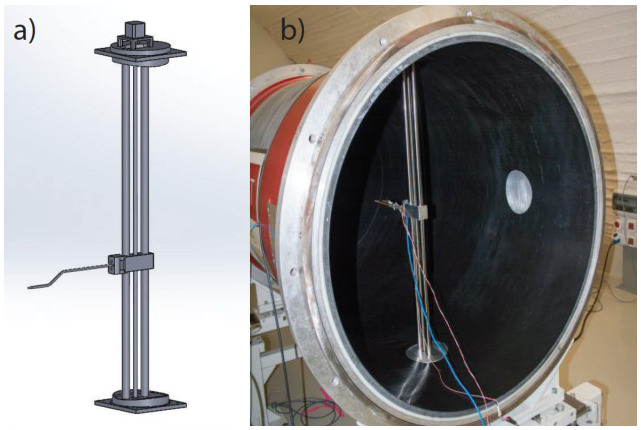

Figure 3. Traversing mechanism mounted vertically in pipe test section and used with Probes 2 and 3; a) CAD model, b) photograph.

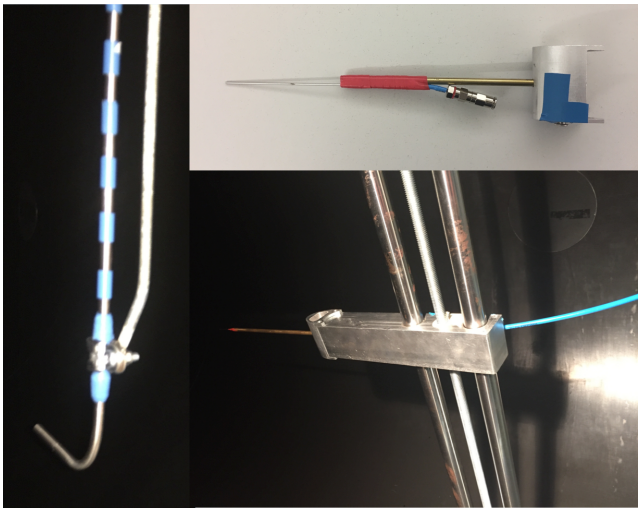

Figure 4. Photographs of Pitot probes used; Left) Pitot-Static Probe 1 with additional support and other means to prevent deflection and vibration during high speed operations, Top-Right) Pitot Probe 3, Bottom-Right) Pitot Probe 2 mounted in traversing holder used with Probes 2 and 3.

readily estimated from it. While this bulk velocity measure my not be as accurate as we require for the centerline velocity measurements, it is continuously measured and recorded by the data acquisition system with the aid of a high accuracy MKS pressure transducer. Comparisons to this bulk velocity proved very important in selecting the best Pitot probe and qualifying its measurements.

II.1 PROBE 1

The first probe tested had an outer diameter of 6mm and an inner hole of 1.8mm. The supporting structure was designed to reduce to a minimum the blockage effect. As a result of the preliminary deflection test, a support system was added to the stem and no influence on the blockage was detected; see left hand side of Fig. 4.

II.2 EFFECT OF LOCATION

A first set of measurements was performed with the probe located at a position 5.5D upstream of the test section, with D being the diameter of the pipe. No differences were found in the results in

terms of bulk and centerline velocity when the location was moved to the test section for the acquisition of a second data set, as Fig. 9 shows. Therefore, all the following tests were conducted with the probe at this latter location.

II.3 STATIC PRESSURE ACQUISITION

Two options were available for the static pressure acquisition in CICLoPE: the static holes from the Pitot probe itself or the pressure ports along the pipe. For each location, there are four ports around the pipe circumference, spaced by 90 degrees. A careful evaluation of the taps was performed, and compared with the static port of the Pitot tube. Tables 1 and 2 summarize the centerline velocities obtained by using each tap at the test section and the holes from the Pitot probe itself. The symmetry of the pipe is confirmed by the absence of differences in the centerline velocities obtained when using the pressure taps, which are, however, slightly lower than the one resulting from using only the Pitot-static probe.

Table 1. Centerline velocity comparison, for 40% Fan speed

Static tap location	Centerline velocity [m/s]
Front	16.83
Top	16.81
Bottom	16.81
Back	16.81
Pitot	16.89

II.4 PROBE 2

A total head probe with a 1mm outer diameter and an inner hole of 0.2mm was mounted on a traverse system spanning the test section. The static pressure was acquired from the tap located at the bottom of the pipe circumference, at the same location as the probe. The results reported in Fig. 11 highlight a problem with Probe 2. For the same bulk velocities as in the previous tests, the centerline value is considerably lower than the one obtained with

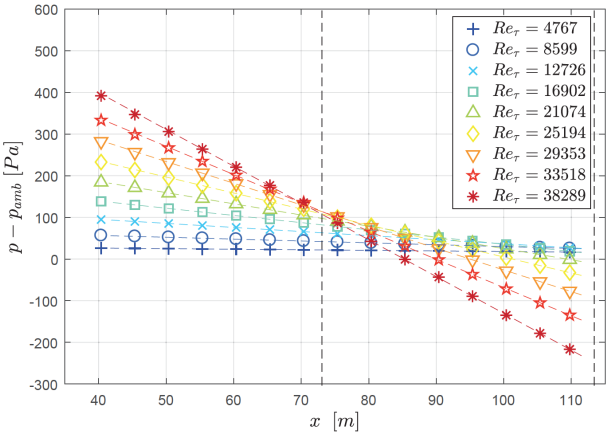

Figure 5. Differential pressure measured in 0.9-m diameter pipe, using outside ambient pressure as reference, as function of distance from pipe entrance, for a range of Reynolds numbers (color dashed lines are linear least squares fits of the data between the two vertical black dashed lines); Reproduction of Figure 3.5 of Fiorini (2017).

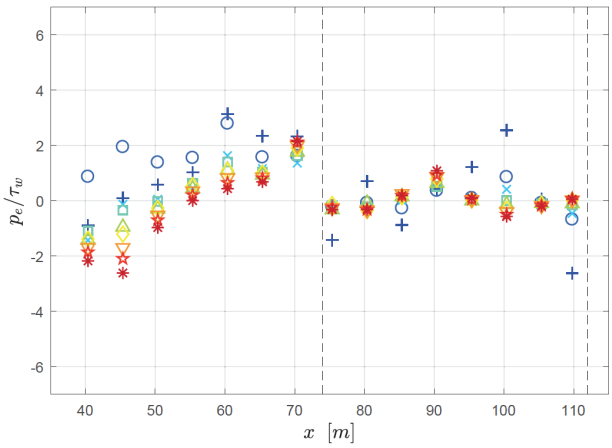

Figure 6. Error between the measured pressure at every tap and the linear fit shown in Figure 5, normalized by the wall friction, with vertical dashed lines represent the region of pipe used for linear fit; Reproduction of Figure 3.6 of Fiorini (2017).

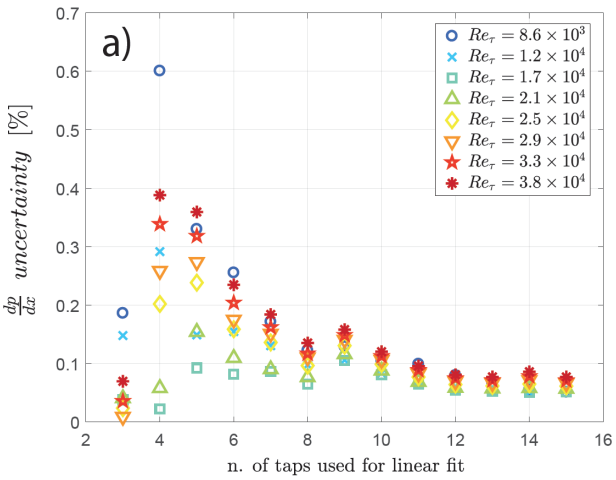

Figure 7. 95% confidence intervals on dp/dx resulting from fit uncertainty, as a function of the number of taps used for the linear fit; Data from Figure 3.4 of Fiorini (2017).

Table 2. Centerline velocity comparison, for 100% Fan speed

Static tap location	Centerline velocity [m/s]
Front	43.36
Top	43.34
Bottom	43.36
Back	43.40
Pitot	43.60

Probe 2. This difference can not be explained by the blockage effect alone. Despite the considerable difference in the supporting structure between this case and the previous', the blockage is only 2.8 %, not enough to affect the centerline velocity to this extent. On the other hand, the geometry of the probe itself can influence the data , and according to McKeon *et al.* (2003) and Chue (1975), the inner diameter of Probe 2, with a $d^+ = 20$ is inside the range where corrections are required. Therefore, a different probe with a larger

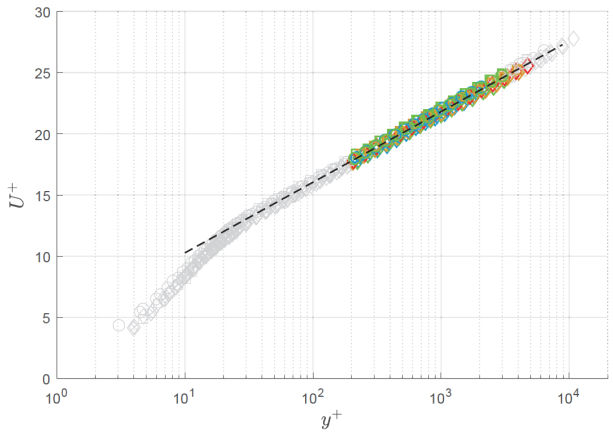

Figure 8. Normalized mean velocity profiles for all of Fiorini (2017) data-sets, excluding ones at lowest Reynolds number, with dashed line depicting log-law resulting from fit of data with $\kappa_{\text{int}} = 0.399$ and $B = 4.50$ (colored symbols are data points in the region $y^+ > 200$ and $y < 0.15R$ used for fitting and grey symbols are data points not used in fit; Reproduction of Figure 4.6 of Fiorini (2017).

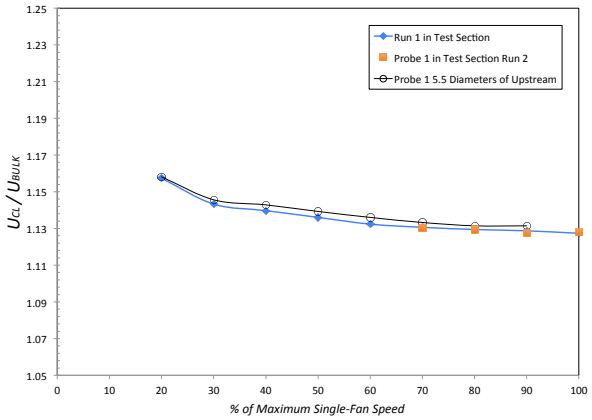

Figure 9. Centerline over bulk velocity ratio, versus fan speed, comparing tests using Pitot-static "Probe 1" at test section, including a repeat run, and 5.5D upstream of test section.

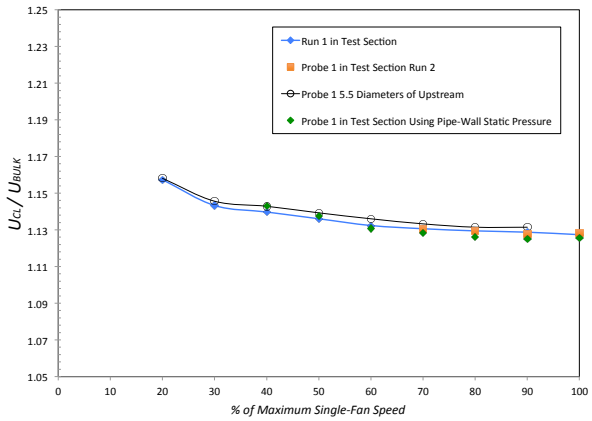

Figure 10. Centerline over bulk velocity ratio versus fan speed results of Figure 9, with additional results utilizing wall static pressure and only total pressure from Pitot-static "Probe 1".

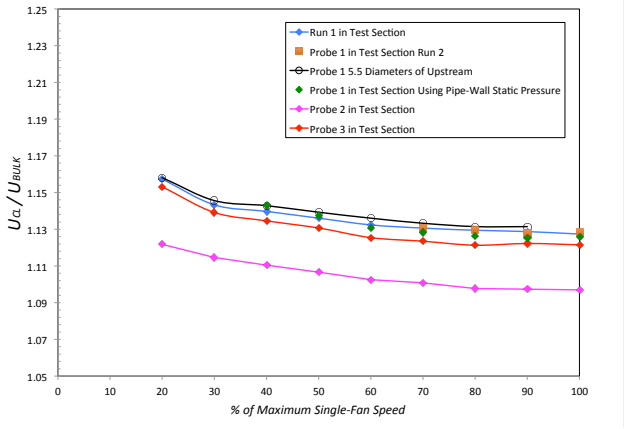

Figure 11. Centerline over bulk velocity ratio versus fan speed results of Figure 10, with additional results utilizing "Probe 2" and "Probe 3".

diameter was used in the following tests.

II.4 PROBE 3

In the last set of measurements, centerline data were acquired with a probe characterized by an outer diameter of 3mm and an inner hole of 1mm. The supporting structure and the static pressure tap were unchanged from the previous set of measurements with Probe 2. The entire range of friction Reynolds numbers from 8 $\times 10^3$ to 40 $\times 10^3$ was explored, and the results are shown in Fig. 11. The outcome is in good agreement with the results obtained during the measurements with Probe 1, and the larger inner diameter solved the problems encountered with the previous set up. The lower value of centerline velocity, due to the blockage effect of the supporting structure explain the position of the blue curve, slightly below the curves referring to Probe 1 data.

III. FRICTION MEASUREMENTS

Wall-friction quantities are required for the scaling of the centerline velocity, since u_τ is found to be the relevant velocity scale both in the inner and outer regions of the flow, according to classical turbulence theory. In the case of a pipe flow, the equilibrium of the forces acting on a volume of fluid of length dx is such that $\tau_w = \frac{dp}{dx}\frac{R}{2}$, with R being the pipe radius. From that, the friction velocity u_τ can be computed, being $u_\tau = \sqrt{\frac{\tau}{\rho}}$.

Since the pressure decreases linearly for a fully-developed turbulent pipe flow, the $\frac{dp}{dx}$ can be found by fitting a line to the experimental data points. An important parameter to consider is the length over which the linear fit is applied, i.e., the number of points used for the fit. An extensive analysis can be found in Fiorini (2017) , where 8 taps covering a distance of 40m from the test section were used, corresponding to $\frac{x}{D} = 44$. In the present work, not only the number of taps contributing to the linear fit was considered, but also the choice and location of the taps. We discovered that a careful selection of the taps used within the range of $\frac{L}{D}$ positions of the taps used by Fiorini (2017) to compute the linear fitting, led to a much better accuracy of the slope of the linear fit, and therefore, the slope of the centerline log law. In Fig. 11, the taps used are highlighted in red whilst the resulting slope is in black.

Comparing Fig. 5 to Fig. 12, the key difference to our approach is not evident. Figure 13 clarifies the merit to our approach, where the deviations between the points not used in the fit (blue) and the fit is two to three times larger than the corresponding difference for the points selected for the fit and shown with red symbols.

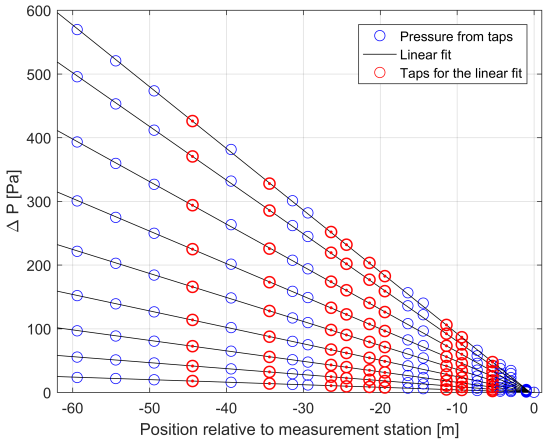

Figure 12. Differential pressure measured in the pipe for Re_τ ranging from 8×10^3 to 40×10^3; red circles are taps used for the linear fit (black line) and blue circles are static pressure from all the taps acquired by the pressure scanner.

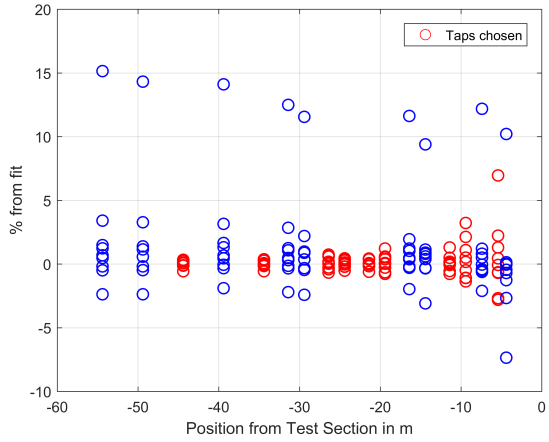

Figure 13. Percent variations from fit in measured differential pressures of Figure 12.

The choice of the final set of points was developed by an iterative procedure over approximately the same range of $\frac{L}{D}$ as that used by Fiorini (2017). While the two farthest downstream points used produce large percentage differences from the fit in Fig. 13, the absolute values of the pressure difference for these points should be kept in mind. The data with blue symbols, not used in the fit, with very large percent deviations from the fit are for the lowest Reynolds number case, where the least accuracy is provided by the pressure scanner. Finally, Fig. 13 confirms the validity of the $\frac{L}{D}$ range used and that fully-developed conditions are reached before the most upstream points of the range, by the very small deviations for the ports around -35m and -45m; i. e., over the Reynolds number range of the current experiments, the flow in the CICLoPE pipe is fully developed within the first 70 diameters of the pipe.

IV. CENTERLINE VELOCITY MEASUREMENTS AND CORRELATIONS

A sample of the final results achieved using Probe 3, and the full range of the current operating conditions at CICLoPE, is shown in Fig. 14. The best logarithmic fit to the data is shown by the red line with error bars of 0.25%. In addition lines are also included

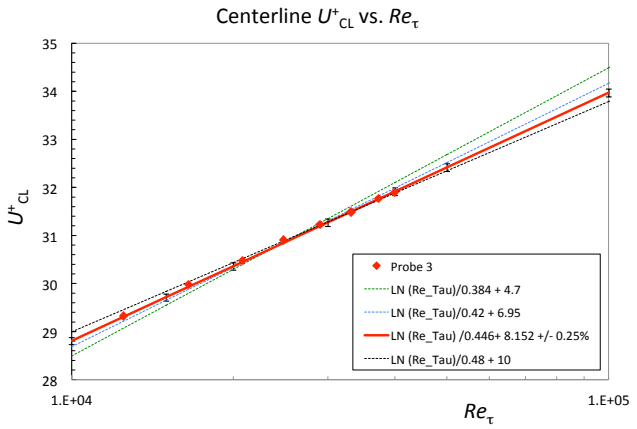

Figure 14. Centerline velocity U^+_{CL} using Probe 3 in test section of pipe, and improved pressure gradient estimates of Figure 12, versus Re_τ; log-law representative of best fit of data with $\kappa_{ext} = 0.446$ and $B = 8.152$ is shown by red line, and three other log laws are shown for reference, with $\kappa_{ext} = 0.42, 0.48$ and the inner-law value of 0.384.

for logarithmic relations with κ_{ext} values of 0.42 (corresponding to the value found by Monkewitz (2017)) and 0.48, with potential to represent this data. From this figure alone, it may be debated what is the best value for κ_{ext} in this range. However, the logarithmic relation also shown in the Fig. 14 with $\kappa = 0.384$ clearly cannot be used to represent these results. This is a very clear demonstration of the separation between κ_{ext} and κ_{int}, even within a somewhat limited range of high Reynolds number in a wall-bounded flow with pressure gradient.

In Fig. 15, the same data are compared with data obtained by Probe 1, data of Fiorini (2017), the original data of Zagarola & Smits (1998), and the results of McKeon *et al.* (2004); note that no significant corrections of Pitot probe data are required on the pipe centerline. We attribute the small difference between the current results and those of Fiorini (2017) from the same facility to two factors: the Pitot probe arrangement differences highlighted in Sec. II, and the improved accuracy in our determination of the pressure gradient discussed in Sec. III.

Finally, in Fig. 16 the full range of data from Zagarola & Smits (1998), and McKeon *et al.* (2004) is included, and further confirms our conclusions. For the highest four Reynolds numbers of the Superpipe data, a Hama-type roughness correction was applied according to Monkewitz (2017).

V. CONCLUSIONS

The asymptotic matching to the "wake", already discussed by Coles (1956) many decades ago, has not received enough attention, nor did his focus on the centerline data of Zagarola & Smits (1998), contained in his unpublished manuscript on turbulent shear flows. Such matching requires that κ_{wall} be the same as κ_{CL} in the expression for the centerline velocity $U^+_{CL} = (1/\kappa_{CL})\ln(\mathrm{Re}_\tau) + C$, but κ_{CL} has consistently remained larger than 0.42. The very recent analysis of Monkewitz (2017) for pipe flow was based on the Superpipe data where κ_{ext} was found to be 0.42. So the question arose in our minds whether the difference between κ_{int} and κ_{ext} is statistically significant. With a high degree of confidence, as demonstrated by Figs. 13 and 14, we find from the present results that this is indeed the case, as κ_{CL} in CICLoPE is found to be $\mathbf{0.446 \pm 0.008}$. Interestingly, this value is very close to the original $\kappa_{CL} = 0.436$ of Zagarola & Smits (1998) for the Superpipe and the value of 0.437 found in the first CICLoPE experiments by Fiorini (2017), as demonstrated in Figs. 15 and 16.

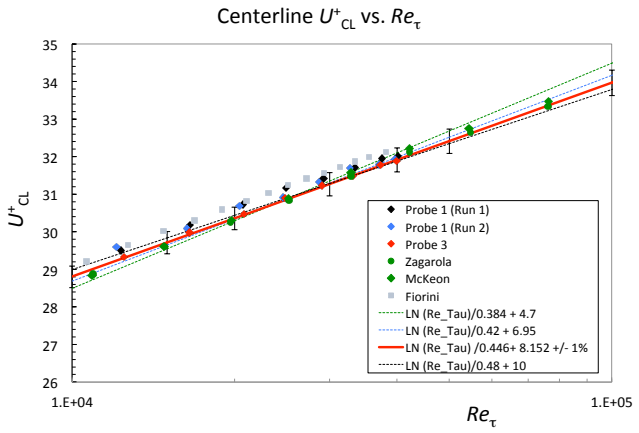

Figure 15. Centerline velocity U^+_{CL} using Probes 1 and 3 in test section of pipe versus Re_τ, compared to earlier data by Fiorini (2017) at CICLoPE with $\kappa_{ext} = 0.437$ and $B = 8.047$, and Superpipe data of Zagarola & Smits (1998) and McKeon *et al.* (2004); the log-law of Monkewitz (2017), a log-law with a larger κ_{ext} of 0.48 and one with slope $\kappa_{int} = 0.384$ are also included.

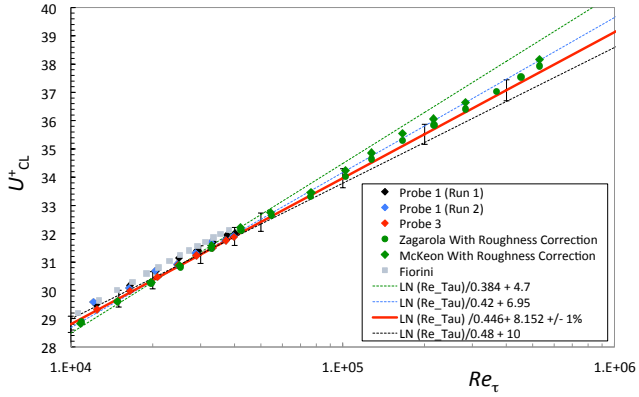

Figure 16. Centerline velocity U^+_{CL} using Probes 1 and 3 in test section of pipe versus expanded range of Re_τ, compared to earlier data by Fiorini (2017) at CICLoPE with $\kappa_{ext} = 0.437$ and $B = 8.047$, and Superpipe data of Zagarola & Smits (1998) and McKeon *et al.* (2004); the log-law of Monkewitz (2017), a log-law with a larger κ_{ext} of 0.48 and one with slope $\kappa_{int} = 0.384$ are also included.

Acknowledgement

We thank the University of Bologna for their support of CICLoPE. The first author also acknowledges some support from the John T. Rettaliata Professorship. Some of the research ongoing at CICLoPE has been supported by the European High performance Infrastructures in Turbulence (EUHIT) project, funded by the European Commission under Grant agreement n.312778 within the FP7.

REFERENCES

Coles, D. E. 1956 The law of the wake in the turbulent boundary layer. *J. Fluid Mech.* **1**, 191–226.

Chue S. H. 1975 Pressure probes for fluid measurement. *Prog. Aerosp. Sci.* **16**, 147-223.

Fiorini, T. 2017 Turbulent pipe flow - high resolution measurements in ciclope. PhD thesis, University of Bologna.

Furuichi, N., Terao, Y., Wada, Y. & Tsuji, Y. 2015 Friction factor and mean velocity profile for pipe flow at high Reynolds numbers. *Phys. Fluids* **27** (9), 095108.

Marusic, I., Monty, J. P., Hultmark, M. & Smits, A. J. 2013 On the logarithmic region in wall turbulence. *J. Fluid Mech. Rapids* **716**, R3–1–R3–11.

McKeon, B. J., Li, J., Jiang, W., Morrison, J. F. & Smits, A. J. 2003 Pitot probe corrections in fully developed turbulent pipe ow. *Meas. Sci and Tech.* **14**, 1449-1458.

McKeon, B. J., Li, J., Jiang, W., Morrison, J. F. & Smits, A. J. 2004 Further observations on the mean velocity distribution in fully developed pipe flow. *J. Fluid Mech.* **501**, 135–147.

Monkewitz, P. A., Chauhan, K. A. & Nagib, H. M. 2007 Self-consistent high-Reynolds-number asymptotics for zero-pressure-gradient turbulent boundary layers. *Phys. Fluids* **19**, 115101.

Monkewitz, P. A. 2017 Revisiting the quest for a universal log-law and the role of pressure gradient in “canonical” wall-bounded turbulent flows. *subm. to Phys. Rev. Fluids; arXiv 1702.03661* .

Örlü, R., Fiorini, T., Segalini, A., Bellani, G., Talamelli, A. & Alfredsson, P. H. 2016 Reynolds stress scaling in pipe flow turbulence - first results from CICLoPE. *Trans. R. Soc. A* **375**, 20160187.

Zagarola, M. V. & Smits, A. J. 1998 Mean-flow scaling of turbulent pipe flow. *J. Fluid Mech.* **373**, 33–79.